BIOLOGY OF REPRODUCTION (2012) **87**(3):56, 1–8
Published online before print 13 June 2012.
DOI 10.1095/biolreprod.112.101832

Characterization of EPPIN's Semenogelin I Binding Site: A Contraceptive Drug Target[1]

Erick J.R. Silva,[2] Katherine G. Hamil, Richard T. Richardson, and Michael G. O'Rand

The Laboratories for Reproductive Biology, Department of Cell & Developmental Biology, University of North Carolina at Chapel Hill, Chapel Hill, North Carolina

ABSTRACT

Epididymal protease inhibitor (EPPIN) is found on the surface of spermatozoa and works as a central hub for a sperm surface protein complex (EPPIN protein complex [EPC]) that inhibits sperm motility on the binding of semenogelin I (SEMG1) during ejaculation. Here, we identify EPPIN's amino acids involved in the interactions within the EPC and demonstrate that EPPIN's sequence C102-P133 contains the major binding site for SEMG1. Within the same region, the sequence F117-P133 binds the EPC-associated protein lactotransferrin (LTF). We show that residues Cys102, Tyr107, and Phe117 in the EPPIN C-terminus are required for SEMG1 binding. Additionally, residues Tyr107 and Phe117 are critically involved in the interaction between EPPIN and LTF. Our findings demonstrate that EPPIN is a key player in the protein-protein interactions within the EPC. Target identification is an important step toward the development of a novel male contraceptive, and the functionality of EPPIN's residues Cys102, Tyr107, and Phe117 offers novel opportunities for contraceptive compounds that inhibit sperm motility by targeting this region of the molecule.

contraception, EPPIN, semenogelin I, spermatozoa

INTRODUCTION

The development of a nonhormonal male contraceptive will provide more contraceptive choices for men and women and contribute to improving human family health. Although progress has been slow for a variety of reasons, a number of promising strategies have appeared in recent years, including therapeutic ultrasound [1], gamendazol [2, 3], retinoic acid antagonist BMS-189453 [4], and the sperm proteins GAPDHS [5], EPPIN [6, 7], and CATSPER [8]. Epididymal protease inhibitor (EPPIN; official symbol SPINLW1) made its debut as a target for male contraception in 2004 with the demonstration that blocking EPPIN's function in nonhuman primates with antibodies led to reversible infertility [7]. EPPIN's function has since been demonstrated to be both antimicrobial [9, 10] and a central hub for a sperm surface protein-protein network (EPPIN protein complex [EPC]) that binds the semen coagulating protein semenogelin I (SEMG1) as part of the complex [11, 12]. EPPIN-SEMG1 binding plays an essential role in reproduction by inhibiting ejaculate sperm motility [13–15] through control of the sperm's internal pH and calcium levels [14, 16]. Moreover, the demonstration that antibodies to EPPIN's C-terminus could substitute for SEMG1 and that the epitope-specific contraceptive antibodies from the infertile nonhuman primates [7] inhibited human sperm motility [14] made it clear that the SEMG1 binding site on EPPIN was a human sperm surface drugable target.

As described previously [6], we used the AlphaScreen assay (Amplified Luminescent Proximity Homogeneous assay) to develop high-throughput screening (HTS) assays to specifically ''hit'' compounds that target EPPIN's SEMG1 binding site. These selected compounds target EPPIN with high affinity, mimic SEMG1 binding, and consequently inhibit human sperm motility. Therefore, a better understanding of the interaction between EPPIN and SEMG1 is an important step for the study of how these compounds bind to EPPIN and for the development of even more effective sperm motility inhibitors. In the present study, we determined EPPIN's amino acid residues involved in its interaction with SEMG1. Our results demonstrated that the sequence C102-P133 within EPPIN's Kunitz domain contains the major binding residues for SEMG1. Moreover, the EPC-associated protein lactotransferrin (LTF) was found to bind the EPPIN sequence F117-P133. The amino acid residues Cys102, Tyr107, and Phe117 that project into the central binding pocket for SEMG1 are critical for EPPIN interaction with SEMG1, whereas residues Tyr107 and Phe117 are further involved in the binding of LTF. Our results characterize EPPIN's residues that could be used as potential targets for improving the rational design of contraceptive drugs.

MATERIALS AND METHODS

Production and Expression of Recombinant Proteins

Recombinant EPPIN and SEMG1 constructs were cloned, expressed, and purified as described in the Supplemental Methods (all Supplemental Data are available online at www.biolreprod.org). Lyophilized full-length recombinant human holo lactotransferrin (LTF; Pro-592) purified from transgenic rice was purchased from Prospec (Ness-Ziona). LTF was resuspended in PBS buffer pH 7.4, aliquoted and stored at −80°C until use. The number of different protein preparations for each recombinant protein used in this study is indicated in Supplemental Table S1.

In Vitro Site-Directed Mutagenesis

Site-directed mutagenesis of wild-type (wt)-EPPIN at residues Cys86, Cys102, Cys110, Cys123, Cys127, Tyr107, and Phe117 to alanine residues was performed using Gene Tailor site-directed mutagenesis system (Invitrogen) according to the manufacturer's instructions. EPPIN mutant designations and mutation sites are shown in Table 1. Mutagenesis products were transformed into DH5α-T^{1R} *Escherichia coli* and positive clones selected, followed by DNA sequencing to confirm the mutation. Recombinant EPPIN mutants were expressed as described in the Supplemental Methods.

[1]Supported by grants HD048843 and HD060494 from the Eunice Kennedy Shriver National Institute of Child Health and Human Development and by grant D43TW-HD00627 from Fogarty International Center Program for Training and Research in Population and Health.
[2]Correspondence: Erick J.R. Silva, The Laboratories for Reproductive Biology, Department of Cell and Developmental Biology, CB# 7090, 206 Taylor Hall, University of North Carolina at Chapel Hill, Chapel Hill, NC, 27599-7090. E-mail: ejrsilva81@gmail.com

Received: 2 May 2012.
First decision: 4 June 2012.
Accepted: 11 June 2012.

eISSN: 1529-7268 http://www.biolreprod.org
ISSN: 0006-3363

TABLE 1. List of EPPIN mutants used in this study.

Mutant designation	Mutation site(s)
mC[1]-EPPIN	C127A
mC[2]-EPPIN	C123A
mC[1,2]-EPPIN	C127A, C123A
mC[1–3]-EPPIN	C127A, C123A, C110A
mC[1–4]-EPPIN	C127A, C123A, C110A, C102A
mC[1–5]-EPPIN	C127A, C123A, C110A, C102A, C86A
mC[4]-EPPIN	C102A
mF-EPPIN	F117A
mY-EPPIN	Y107A
mYF-EPPIN	F117A, Y107A
mFC[1–4]-EPPIN	F117A, C127A, C123A, C110A, C102A
mYC[1–4]-EPPIN	Y107A, C127A, C123A, C110A, C102A
mYFC[1–4]-EPPIN	F117A, Y107A, C127A, C123A, C110A, C102A

AlphaScreen Assay

The AlphaScreen assay is a bead-based technology that allows the study of different types of biomolecular interactions [for review, see Eglen et al. 17]. When acceptor and donor beads are brought together ($\leq$200 nm) by the interacting molecules, the excitation of the donor beads generates singlet-state oxygen molecules ($t_{1/2} \sim 4$ μsec), which initiate a chemiluminescent reaction in the acceptor bead that emits light at 520–620 nm. The AlphaScreen assay was performed in white opaque 384-well microplates (OptiPlate-384; PerkinElmer) in a final volume of 20 or 30 μl, depending on the experiment as indicated. Unless otherwise stated, all dilutions were made in assay buffer (100 mM Tris-HCl, 0.1% bovine serum albumin, wt/vol, 0.01% casein, wt/vol, 0.01% Tween-20, vol/vol, pH 8.0). In the AlphaScreen IgG (Protein A) detection kit (PerkinElmer), acceptor beads were conjugated with Protein A and donor beads with streptavidin. The experiments were carried out at room temperature and under subdued lighting.

Each recombinant EPPIN construct (wild-type, truncations, and mutants) was preincubated with anti-EPPIN Q20E antibody and Protein A acceptor beads for 30 min. In parallel, recombinant biotinylated (bt)-SEMG1 or bt-LTF was preincubated with streptavidin donor beads under the same conditions. Equal volumes of each EPPIN/Q20E/Protein A acceptor beads and bt-SEMG1/streptavidin donor beads or bt-LTF/streptavidin donor beads were pipetted into the plate wells. The final concentration of assay components was 58 nM EPPIN, 1 nM bt-SEMG1 or 4 nM bt-LTF, 2 nM Q20E antibody, and 10 μg/ml beads. Each set of samples was pipetted in at least four replicates. Plates were covered with top seal and transferred to a Synergy 2 Multiplatform automated plate reader (Biotek). After shaking for 2 min, plates were read every 2 h during 16 h: excitation using a 680/30 filter and emission using a 570/100 filter and data acquired using a modified AlphaScreen protocol in the Gen5 software (Biotek). A total of nine time points were generated during each experiment. Negative controls were performed under the same conditions in the absence of EPPIN, bt-SEMG1, or bt-LTF and in the presence of beads only. A specific signal for each time point was calculated by subtracting the background signal (obtained in the absence of bt-SEMG1 or bt-LTF) from its respective total signal. To monitor assay sensitivity and robustness, signal-to-background (S/B) ratios and Z' values were calculated as previously described [18].

Concentration-Response and Competition Experiments

Concentration-response experiments were carried out as described above using increasing concentrations of wt-EPPIN (1 nM–1 μM) in the presence of constant concentrations of bt-SEMG1 (0.5–4 nM) or bt-LTF (4–8 nM) in a 20 μl-assay volume. Similarly, increasing concentrations of bt-SEMG1 (0.1 pM–1 nM) or bt-LTF (3 pM–8 nM) were incubated in the presence of a constant concentration of EPPIN (58 nM). The bead concentration was 10 μg/ml. Specific counts for each data point were calculated as described above and used for the determination of EC_{50} values by nonlinear regression curve fitting.

For competition experiments, wt-EPPIN (10 or 30 nM) and bt-SEMG1 (1 nM) or bt-LTF (2 nM) were incubated in the presence of increasing concentrations of nonbiotinylated SEMG1 (10 pM–150 nM) or LTF (100 pM–600 nM) in a 30 μl-assay volume. In this case, wt-EPPIN and bt-SEMG1 or bt-LTF were preincubated with their respective beads as described above, and the solutions were pipetted into the plate wells in the following order: 5 μl competitor protein dilutions, 10 μl of wt-EPPIN/Q20E/Protein A acceptor beads, and 15 μl of bt-SEMG1/streptavidin donor beads or bt-LTF/streptavidin donor beads. The bead concentration was 15 μg/ml. A specific signal for each competitor concentration point was calculated as described above. The IC_{50} values were calculated by nonlinear regression curve fitting using the normalized data as a percentage of the specific binding in the absence of competitor. AlphaScreen TruHits assay was used as a positive control (for nonspecific effects) under the same conditions as described in the Supplemental Methods.

EPPIN Homology Modeling

Three-dimensional homology models for the EPPIN C-terminal region (K73-P133) were built using the SWISS-MODEL Workspace [19–21]. After template identification, we chose four templates (Protein Data Bank identification [PDB ID]) based on the percentage of sequence identity to EPPIN C-terminus: bovine trypsin inhibitor (aprotinin; 1bpiA), boophilin (2odyE), textilinin-1 (3bybB), and alpha3 chain of human type VI collagen (1kthA). EPPIN structural models were then generated using the described templates as reference structures. We compared the quality of the resulting three-dimensional models using QMEAN Z-score (global quality of the generated model) [22]. We selected the model with the highest QMEAN Z-score and then created EPPIN C-terminal model figures using Swiss-PDB Viewer 4.04 (Swiss Institute of Bioinformatics) and rendered with POV-Ray 3.6 (Persistence of Vision Raytracer Pty Ltd).

Statistical Analysis

Results were expressed as mean $\pm$ standard deviation (SD) or standard error of the mean (SEM) from the indicated number of independent experiments. For statistical significance, one-way analysis of variance (ANOVA) followed by the Tukey-Kramer test was performed when more than two groups were compared, whereas the Student *t*-test was used to compare two groups; $P < 0.05$ was considered statistically significant. Statistical comparisons were performed using Prism 5.0 software.

RESULTS

Characterization of bt-SEMG1 or bt-LTF Binding to wt-EPPIN

We previously demonstrated that EPPIN coats the surface of human spermatozoa [12, 15, 23], where it is a central player in a network of protein-protein interactions with SEMG1 and LTF as part of the EPC [11, 12]. In the present study, we used the AlphaScreen assay to determine the EPPIN sequences and amino acid residues required for binding to SEMG1 and LTF. We first characterized the binding of recombinant bt-SEMG1 or bt-LTF to recombinant wt-EPPIN in this assay (see Supplemental Results and Supplemental Fig. S1). The binding of bt-SEMG1 or bt-LTF to wt-EPPIN was time dependent (Fig. 1A). An increase in the signal was observed during the first 6 h of incubation, reaching a maximum plateau 8 h after incubation. The maximum signal was maintained for at least 16 h after incubation (Fig. 1A), demonstrating that the interaction between wt-EPPIN and bt-SEMG1 or bt-LTF is highly stable. We performed all further analyses using the signal measured 16 h after the start of incubation.

Concentration-response experiments performed using increasing concentrations of wt-EPPIN in the presence of three different concentrations of bt-SEMG1 showed that the binding of wt-EPPIN to bt-SEMG1 was saturable (Fig. 1B, left panel). The calculated EC_{50} (95% confidence interval) was 26.4 (23.3–29.9), 18.4 (17.2–19.5), and 37.2 (33.7–40.9) when wt-EPPIN was titrated in the presence of 0.5 nM, 1 nM, and 4 nM bt-SEMG1, respectively. Moreover, S/B ratios and Z' values varied depending on the bt-SEMG1 concentration, achieving optimal conditions when 58 nM wt-EPPIN and 1 nM bt-SEMG1 were used (Supplemental Table S2). When increasing concentrations of bt-SEMG1 were incubated in the presence of 58 nM wt-EPPIN (Fig. 1C, left panel), the calculated EC_{50} was 0.11 nM (0.1–0.13 nM), and an optimal S/B ratio of 174.6 and Z' value of 0.87 were obtained using 1 nM bt-SEMG1.

We observed no saturation when increasing concentrations of wt-EPPIN were incubated in the presence of 4 and 8 nM bt-

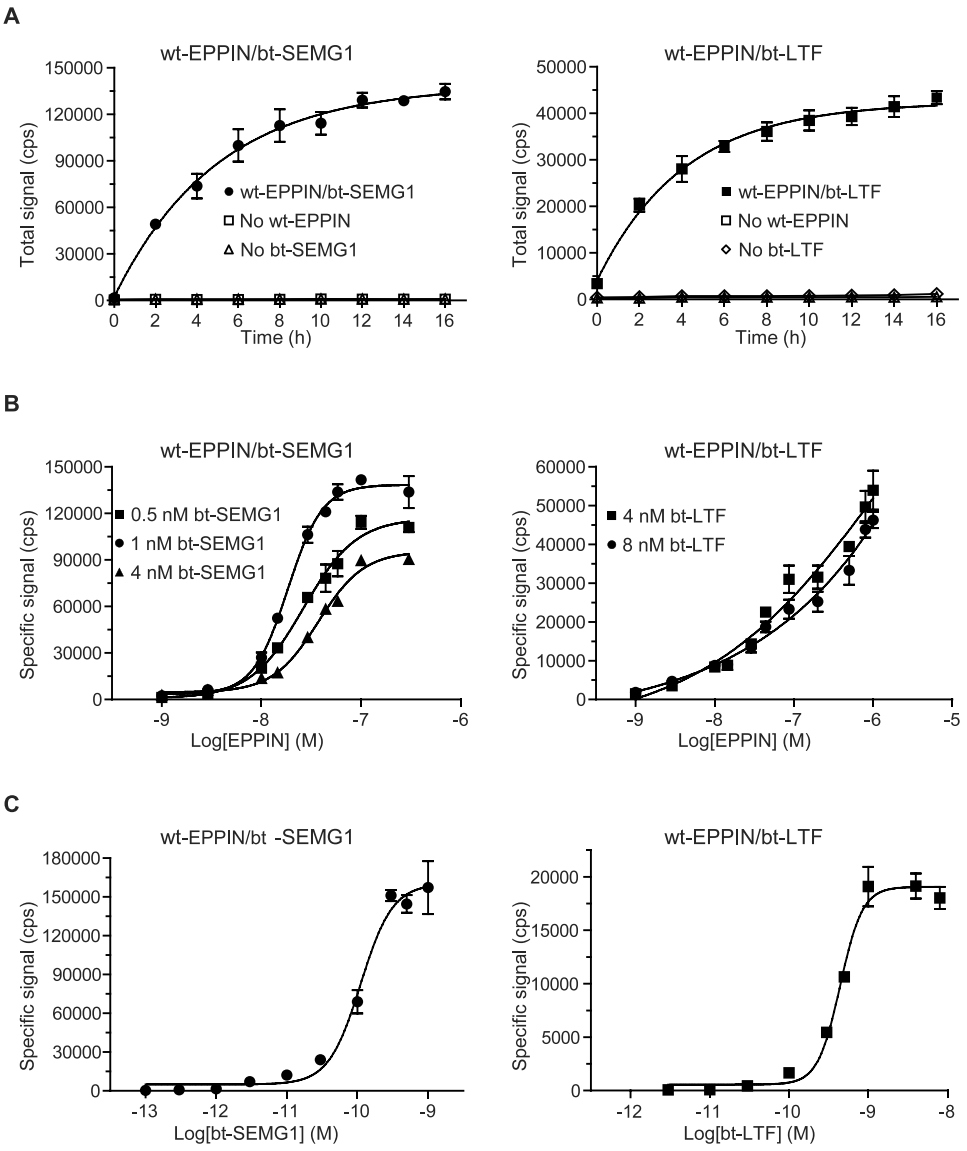

FIG. 1. Characterization of the interaction between wt-EPPIN and bt-SEMG1 or bt-LTF by AlphaScreen assay. **A**) wt-EPPIN was incubated with bt-SEMG1 (left panel) or bt-LTF (right panel) in a time-course experiment. Background signal was detected when beads were incubated in the absence of wt-EPPIN, bt-SEMG1, or bt-LTF. Data points represent mean ± SD of total signal from a representative experiment of four experiments, each performed in four replicates. **B**) Concentration-response curve for wt-EPPIN in the presence of constant concentrations of bt-SEMG1 (left panel) or bt-LTF (right panel). **C**) Concentration-response curve for bt-SEMG1 (left panel) or bt-LTF (right panel) in the presence of a constant concentration of wt-EPPIN. Specific signal for each data point was determined by subtracting the background signal from total signal. Data points in **B** and **C** represent mean ± SD of specific signal from a representative experiment of three experiments, each performed in four replicates. cps = counts per second.

LTF even when the concentration of wt-EPPIN was increased up to 1 μM (Fig. 1B, right panel). However, the titration of bt-LTF in the presence of 58 nM wt-EPPIN showed a maximum plateau within 1–8 nM bt-LTF (Fig. 1C, right panel). Under these conditions, the calculated EC_{50} for bt-LTF was 0.43 nM (0.41–0.48 nM), and an optimal S/B ratio of 29.9 and Z′ value of 0.81 were obtained using 4 nM bt-LTF. These results demonstrated the robustness, sensitivity and reliability of the assay to measure the binding of bt-SEMG1 or bt-LTF to wt-EPPIN.

Effect of Nonbiotinylated SEMG1 and LTF on the Binding of bt-SEMG1 or bt-LTF to wt-EPPIN

We investigated the ability of nonbiotinylated SEMG1 and LTF to displace bt-SEMG1 or bt-LTF from their respective binding sites on wt-EPPIN. As expected, neither of the nonbiotinylated proteins had an effect on the signal in the absence of bt-SEMG1 or bt-LTF (Supplemental Table S3). SEMG1 competed with bt-SEMG1 for binding wt-EPPIN in a concentration-dependent manner with a calculated IC_{50} value (95% confidence interval) of 5.2 nM (3.9–6.9 nM; Fig. 2A). Similarly, LTF competed with bt-LTF with an IC_{50} of 4.8 nM (3.5–6.5 nM; Fig. 2B).

Interestingly, cross-competition experiments demonstrated that SEMG1 and LTF inhibited the binding of bt-LTF and bt-SEMG1, respectively, to wt-EPPIN (Fig. 2, A and B). The calculated IC_{50} values were 3.7 nM (3.2–4.4 nM) for LTF-induced inhibition of wt-EPPIN/bt-SEMG1 binding and 27.8 nM (11.7–65.7 nM) for SEMG1-induced inhibition of wt-EPPIN/bt-LTF binding. The TruHits assay performed in the presence of the same concentrations of SEMG1 or LTF

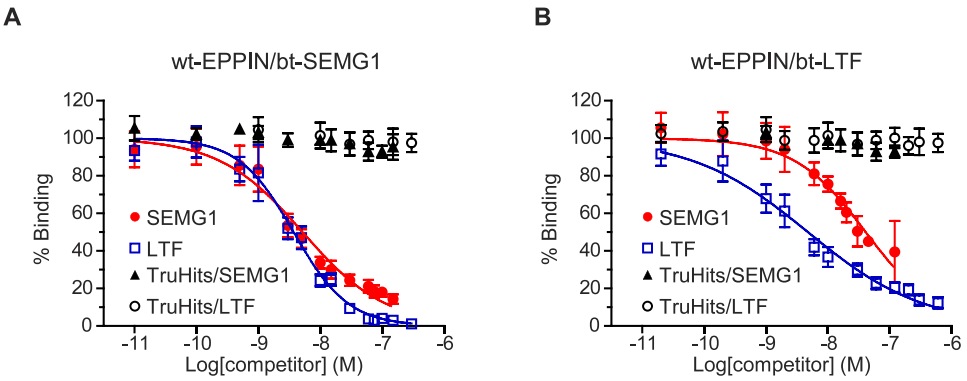

FIG. 2. Displacement of bt-SEMG1 (**A**) or bt-LTF (**B**) from their respective binding sites on wt-EPPIN by nonbiotinylated SEMG1 or LTF; wt-EPPIN was incubated with bt-SEMG1 or bt-LTF in the presence of increasing concentrations of SEMG1 or LTF. Specific signal for each data point was determined by subtracting the background signal from total signal and then normalized as percentage of specific signal in the absence of SEMG1 or LTF. Control experiments were performed with AlphaScreen TruHits in the presence of SEMG1 of LTF under similar conditions. Data are expressed as mean ± SD from three independent experiments, each performed in four replicates.

confirmed that their inhibitory effect on EPPIN/bt-LTF and EPPIN/bt-SEMG1 binding, respectively, was specific (Fig. 2, A and B). These results suggested that SEMG1 and LTF compete for binding to EPPIN.

Effect of Sequential C-terminal Truncations of EPPIN on Its Binding to bt-SEMG1 or bt-LTF

Previously, we demonstrated that the C-terminal fragment of EPPIN containing the Kunitz domain and corresponding to amino acid residues D75-P133 was responsible for its interaction with SEMG1 [12]. To determine which region within the C-terminus of EPPIN is involved in the binding to SEMG1, we produced three sequential EPPIN C-terminal truncations lacking residues F117-P133 ($EPPIN^{22–116}$), C102-P133 ($EPPIN^{22–101}$), and C86-P133 ($EPPIN^{22–85}$; Fig. 3A). We observed a significant reduction (mean ± SD; $P < 0.01$) in the specific signal by 68.7% ± 5.2 for $EPPIN^{22–116}$, 77.9% ± 3.8 for $EPPIN^{22–101}$, and 97.9% ± 3.5 for $EPPIN^{22–85}$ in comparison to the specific signal detected with the binding of wt-EPPIN to bt-SEMG1 (Fig. 3B, left panel).

Next, we tested the binding of each EPPIN C-terminal truncation to bt-LTF under similar conditions. In this situation, the total signal observed when $EPPIN^{22–116}$, $EPPIN^{22–101}$, and $EPPIN^{22–85}$ were incubated with bt-LTF was only slightly above the background (Supplemental Table S4). When compared to wt-EPPIN, the specific signal observed with all the truncations was reduced to less than 1% (Fig. 3B, right panel). Taken together, these results demonstrated that the amino acid residues C102-P133 and F117-P133 within the EPPIN C-terminal region contain the major binding sites for SEMG1 and LTF, respectively. Furthermore, the results indicated that these binding sites partially overlap, supporting the previous result showing that SEMG1 and LTF compete for wt-EPPIN.

Effect of Point Mutations in EPPIN's C-Terminal Region on Its Binding to bt-SEMG1 or bt-LTF

In order to map the EPPIN C-terminal amino acid residues that are critical for binding to SEMG1 and LTF, we produced EPPIN mutants by site-directed mutagenesis (Table 1). Considering the previous observation that Cys239 in the SEMG1 sequence was necessary for interaction with EPPIN [12], we first evaluated the effect of sequential mutations on EPPIN cysteine residues 86, 102, 110, 123, and 127. We observed that single mutations C127A (mC^1-EPPIN) and C123A (mC^2-EPPIN), as well as double C127A:C123A ($mC^{1,2}$-EPPIN) and triple C127A:C123A:C110A ($mC^{1–3}$-EPPIN) mutations, had no effect on EPPIN binding to bt-SEMG1 when compared to the wild type (Fig. 4A). However, we detected a significant reduction in the signal by 51.3% ± 6.1 (mean ± SD; $P < 0.01$) when the EPPIN mutant containing quadruple mutation C127A:C123A:C110A:C102A ($mC^{1–4}$-EPPIN) was compared to wt-EPPIN (Fig. 4A). To investigate whether EPPIN's Cys102 residue alone could disrupt the binding of bt-SEMG1, we produced an EPPIN mutant containing a single mutation C102A (mC^4-EPPIN). Our results demonstrated a significant reduction in the signal by 42.2% ± 3.0 when mC^4-EPPIN was compared to the wild type (Fig. 4A), indicating that the residue Cys102 of EPPIN is involved in the binding of SEMG1. Furthermore, we observed no additional reduction in the signal when the EPPIN mutant containing an additional mutation on residue Cys86 to alanine (quintuple mutant, $mC^{1–5}$-EPPIN) was compared to $mC^{1–4}$-EPPIN and mC^4-EPPIN (Fig. 4A).

To further characterize the EPPIN amino acids involved in binding to SEMG1, we developed a homology model of EPPIN's C-terminus (residues K73-P133; Fig. 5). We selected the serine protease inhibitor aprotinin (bovine trypsin inhibitor; PDB ID 1bpiA [24]) as the reference structure because it provided a model with the highest QMEAN Z-score (−0.68) among the reference protein structures tested (Supplemental Table S5). The EPPIN C-terminus three-dimensional model contains the three-disulfide bridges and secondary-structure arrays typical of the Kunitz domain [25] (Fig. 5B). In this model, we observed that the aromatic side chains of residues Tyr107 and Phe117 were located at the N- and C-terminus, respectively, of a loop that is part of the epitope of contraceptive antibodies from infertile nonhuman primates [7] and the binding sequence for SEMG1 (Fig. 5C). Therefore, we performed mutations on these residues: Tyr107 and/or Phe117 to alanine (Table 1). We observed that Y107A (mY-EPPIN) and F117A (mF-EPPIN) mutations significantly reduced the binding to bt-SEMG1 by 68.4% ± 3.8 and 68.7% ± 3.8 ($P < 0.01$), respectively, in comparison to wt-EPPIN (Fig. 4B). The specific signal was reduced to a similar level when the double mutation Y107A:F117A (mYF-EPPIN) was tested (65.8% ± 4.3; Fig. 4B). Similarly, we observed a significant reduction in the specific signal by 66.4% ± 4.7, 66.8% ± 5.0, and 69.0% ± 3.8 when mutations Y107A ($mYC^{1–4}$-EPPIN), F117A ($mFC^{1–4}$-EPPIN), and

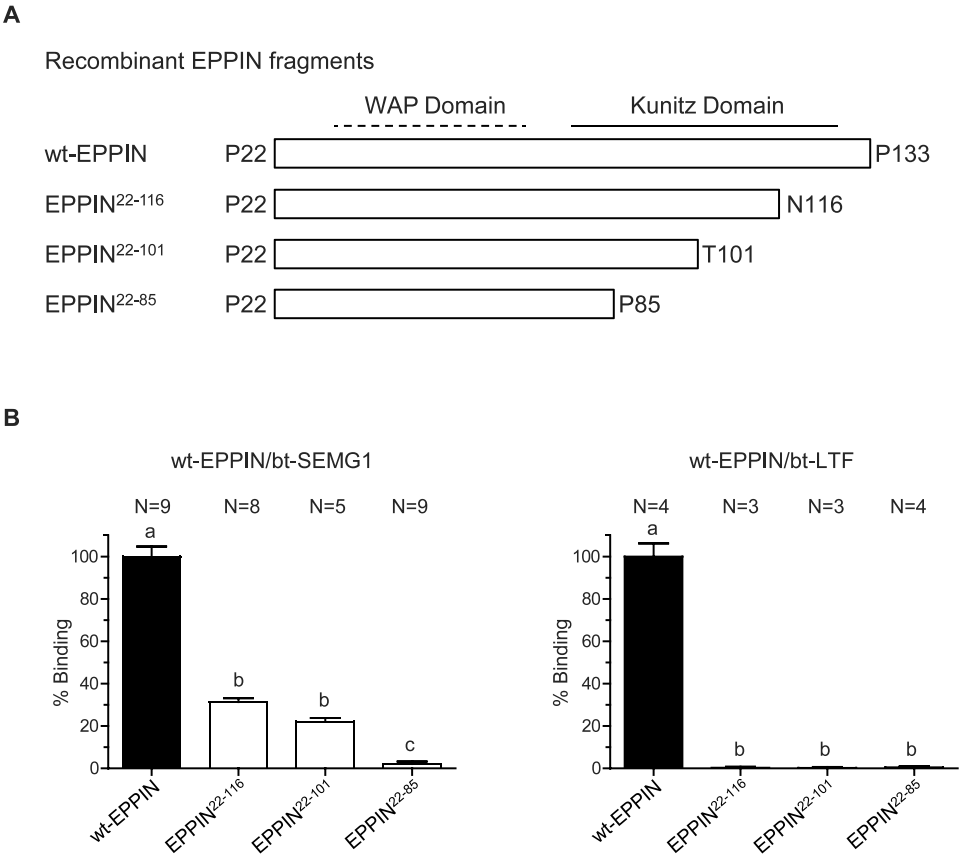

FIG. 3. Effect of sequential C-terminal truncations of EPPIN on bt-SEMG1 or bt-LTF binding. **A**) Schematic representation of recombinant EPPIN fragments P22-P133 (wt-EPPIN; full length lacking the signal peptide) and sequential C-terminal truncations P22-N116, P22-T101, and P22-P85. WAP (N-terminal) and Kunitz (C-terminal) domains are indicated by dashed and solid lines, respectively. **B**) EPPIN constructs were incubated with bt-SEMG1 (left panel) or bt-LTF (right panel). Specific signal for each EPPIN construct was determined by subtracting the background signal from total signal and then normalized as percentage of specific signal for wt-EPPIN. Data are expressed as mean ± SEM from the indicated number of experiments, each performed in six replicates. Different letters in the same bar graphic mean statistically significant differences (ANOVA, followed by Tukey test; $P < 0.01$).

Y107A:F117A (mYFC$^{1-4}$-EPPIN), respectively, were associated with quadruple Cys-mutation C127A:C123A:C110A:-C102A (Fig. 4B). Therefore, the reduction in the signal caused by mutations Y107A and/or F117A on EPPIN sequence was not affected by mutations on the indicated cysteine residues. Consequently, we conclude that residues Cys102, Tyr107, and Phe117 in the C-terminal region of EPPIN play a major role in the binding of SEMG1.

In parallel, we investigated the binding of EPPIN mutants to bt-LTF. In this case, we tested only mutants mC^1-EPPIN (C127A), mC^2-EPPIN (C123A), mF-EPPIN (F117A), and mC^{1,2}-EPPIN (C127A:C123A) because they contain mutations in residues that are part of the F117-P133 fragment, which was shown to be critical for EPPIN interaction with LTF (Fig. 3B, right panel). We observed no difference in the signal when EPPIN mutants mC^1-EPPIN, mC^2-EPPIN, and mC^{1,2}-EPPIN were compared to wt-EPPIN (Fig. 4C). However, we detected a significant reduction of 73.7% ± 3.6 ($P = 0.002$) in the signal when mF-EPPIN was compared with wt-EPPIN (Fig. 4D). These results indicated that EPPIN's residues Tyr107 and Phe117 are critical for the binding of LTF.

DISCUSSION

In the present study, amino acids C102-P133 and F117-P133 of the EPPIN C-terminus were identified as containing the major binding sites for SEMG1 and LTF, respectively. Within these sequences, residues Cys102, Tyr107 and Phe117 play key roles in these interactions. Therefore, our results suggest that EPPIN's residues Cys102, Tyr107, and Phe117 should be explored as targets for contraceptive drug design.

We developed and validated a nonradioactive quantitative bioassay for evaluating EPPIN interactions with SEMG1 and LTF using the AlphaScreen technology. As indicated by Z′ values greater than 0.7, high S/B ratios, and low variability, the developed assay was robust and sensitive, making it suitable for HTS purposes [26, 27]. In fact, we have successfully used this assay in a series of HTS studies to identify lead compounds that block SEMG1 binding to EPPIN [6].

Titration curves demonstrated that the binding of bt-SEMG1 and bt-LTF to wt-EPPIN was concentration dependent and saturable. Interestingly, a plateau was not reached when wt-EPPIN was titrated in the presence of bt-LTF, which may indicate the capacity of LTF to bind multiple EPPIN molecules. The time-dependent pattern of the binding of bt-SEMG1 and bt-LTF to EPPIN (Fig. 1A) suggests that in our assay conditions these interactions have a slow kinetics but were highly stable. We noted that the order of addition of the assay components did not affect the observed time-course pattern. We do not have an explanation for this observation; however, the interaction between these proteins may have a slow association rate and a high on/off ratio. Support for this hypothesis is provided by studies demonstrating a time-dependent effect of SEMG1 on binding to spermatozoa and reducing their forward motility [13, 14]. However, we cannot rule out the possibility that it may take longer for EPPIN and/or

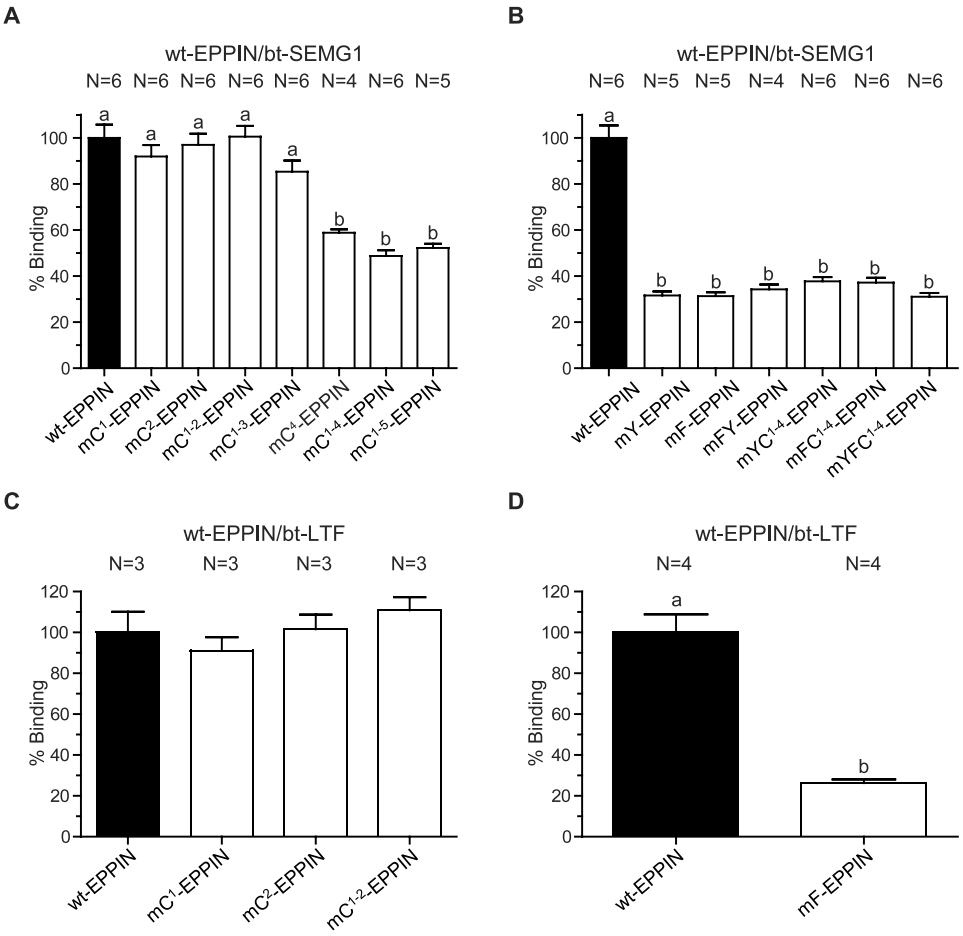

FIG. 4. Effect of point mutations on EPPIN on bt-SEMG1 (**A** and **B**) or bt-LTF (**C** and **D**) binding. EPPIN mutant designations and mutation sites are shown in Table 1. EPPIN constructs were incubated with bt-SEMG1 or bt-LTF. Specific signal for each EPPIN construct was determined by subtracting the background signal from total signal and then normalized as percentage of specific signal for wt-EPPIN. Data are expressed as mean ± SEM from the indicated number of experiments, each performed in six replicates. Different letters in the same bar graphic mean statistically significant differences (ANOVA, followed by Tukey test, $P < 0.01$, for **A**–**C**, or Student *t*-test, $P = 0.0002$, for **D**).

its binding partners to achieve the proper folding that is required for their interaction in the assay conditions.

As expected, competition experiments demonstrated that nonbiotinylated SEMG1 and LTF effectively inhibited the interaction between their biotinylated counterparts to wt-EPPIN with calculated IC_{50} in the low nanomolar range, confirming the specificity of the assay. LTF and SEMG1 specifically inhibited the binding of wt-EPPIN to bt-SEMG1 and bt-LTF, respectively, indicating that there are amino acids in the EPPIN Kunitz domain simultaneously involved in both interactions. Indeed, binding studies using C-terminal truncated EPPIN (Fig. 3) suggested that the major binding sites for SEMG1 and LTF on EPPIN partially overlap. SEMG1 binds to EPPIN's C-terminal sequence C102-P133, while LTF binds to F117-P133. These results confirmed the previous observation that the EPPIN Kunitz domain is critical for its interaction with SEMG1 [12, 14] and further demonstrated that it contains a binding site for LTF. Modulatory sites involved in the inhibition of proteases PSA (Leu87 [28]) and elastase [9] were identified within EPPIN's Kunitz domain, suggesting its critical role in the multifunctional properties of EPPIN.

Our results demonstrated that sequential point mutations in consecutive cysteine residues 127, 123, and 110 to alanine did not affect the binding of SEMG1 or LTF to EPPIN. Although these cysteine residues could be important to stabilize the three-dimensional structure of EPPIN's Kunitz domain, they are unlikely to be involved in the interactions within the EPC. On the other hand, the single point mutation of Cys102 to alanine reduced EPPIN binding to SEMG1 by approximately 45% of the wild type, suggesting that it plays a critical role in EPPIN-SEMG1 interaction. Since previous studies demonstrated that reduction and carboxymethylation of SEMG1's unique cysteine residue (Cys239) blocks the binding of EPPIN [12], it is possible that a disulfide link occurs between SEMG1's Cys239 and EPPIN's Cys102 residue. The fact that EPPIN containing C102A mutation was still able to bind SEMG1 indicated that other types of interactions must be involved in EPPIN-SEMG1 binding. Additional studies will be required to confirm this hypothesis, including the identification of other amino acid residues, in addition to Cys239, in SEMG1 that are involved in its interaction with EPPIN.

To visualize the EPPIN binding site for SEMG1 and LTF, we used the SWISS-MODEL Workspace [19–21] to build a three-dimensional model of the EPPIN C-terminus (Fig. 5) because a crystal structural is not available for EPPIN. The bovine trypsin inhibitor [24] was chosen as the reference structure because it has greater than 40% sequence identity with EPPIN's C-terminus and provided a model with the best global quality estimation among the generated models. The QMEAN Z-score of −0.68 for this model indicated that the structure was within the good-quality range for theoretical protein structure models [22]. The EPPIN C-terminal model

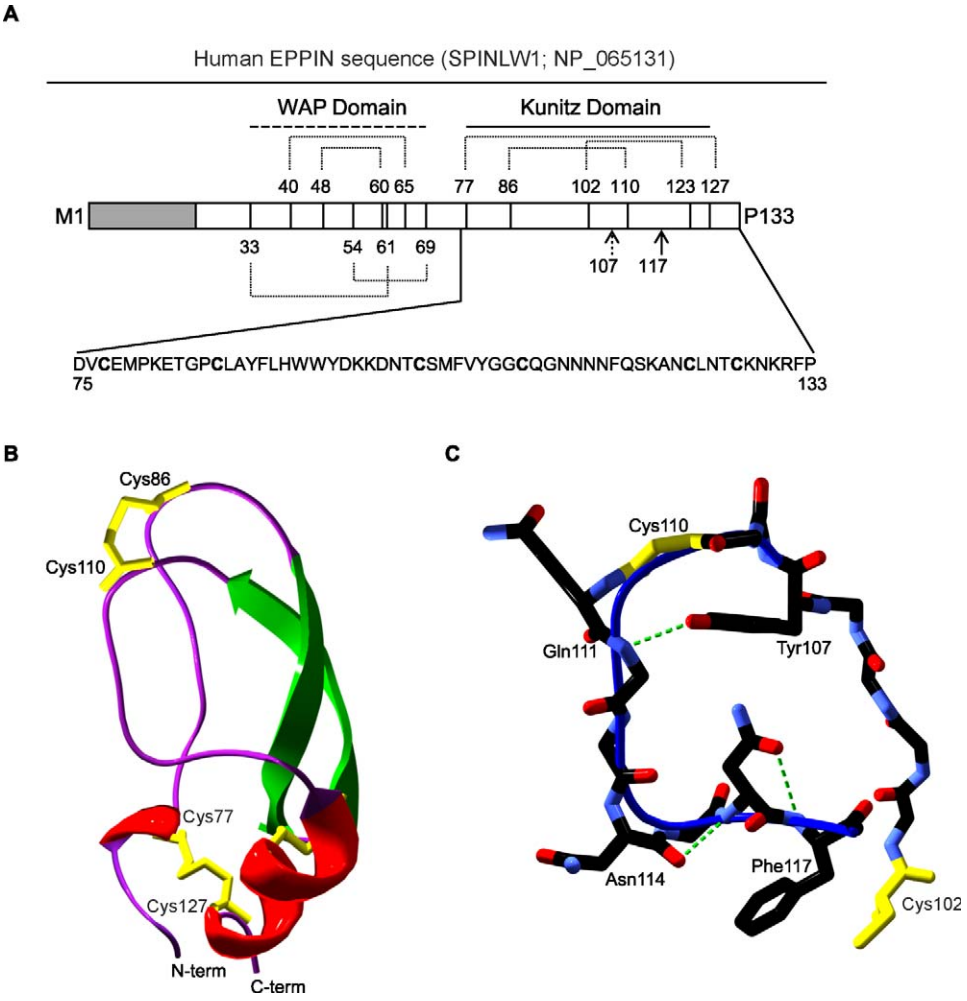

FIG. 5. Three-dimensional model of EPPIN C-terminal region (K73-N129) generated on SWISS-MODEL Workspace [19–21] using bovine trypsin inhibitor (PDB ID 1bpiA) as template. **A**) Schematic representation of human EPPIN sequence containing both WAP (N-terminal) and Kunitz (C-terminal) domains. Cysteine residues are indicated by vertical lines. Residues Tyr107 and Phe117 are indicated by dotted and solid arrows, respectively. Predicted disulfide bonds are illustrated by dotted lines between the indicated cysteine residues in both WAP and Kunitz domains. EPPIN C-terminal amino acid residues D75-P133 containing the binding site for SEMG1 and LTF are shown. Gray box indicates signal peptide. **B**) Ribbon structure of EPPIN's Kunitz domain showing alpha helix (red), beta strands (green), loops (purple), and three disulfide bonds (yellow). **C**) Zoom of the loop (blue) containing residues Tyr107 and Phe117 that are critically involved in EPPIN's interaction with SEMG1 and LTF. The backbone of the amino acid residues within this loop is shown. Residues Cys102 and Cys110 are shown in yellow. Residues Gln111, and Asn114 are also indicated. Hydrogen bonds within this region are illustrated (dotted green lines).

allowed us to visualize the typical distribution of the three disulfide bonds present in the Kunitz domain [25] (Fig. 5, A and B). Within this three-dimensional model, we noted the presence of two large hydrophobic residues (Tyr107 and Phe117), each one located in the N-terminus and C-terminus, respectively, of a loop that contains a repeat of asparagine residues (N113-N116) (Fig. 5, A and C). It is worth noting that residues Tyr107 and Phe117 are highly conserved among proteins containing the Kunitz-type protease inhibitor motif, including those with high levels of expression in the male reproductive tract, such as EPPIN [23, 29], WFDC6, WFDC8, [30] and the recently described SPINT3, SPINT4, and SPINT5 [31]. Our results demonstrated that single point mutations in either of these amino acids reduced EPPIN binding to SEMG1 or LTF by approximately 70% when compared to the wild type, leading to the conclusion that they are critically involved in the macromolecular interactions within the EPC.

Residues Tyr107 and Phe117 are part of the epitope recognized by the contraceptive antibodies of the infertile male monkeys [7] and the epitope-specific anti-EPPIN antibody S21C (SMFVYGGCQGNNNNFQSANC), both of which cause a dramatic inhibitory effect on human sperm motility by mimicking the effects of SEMG1 after it binds to EPPIN [6, 14, 16]. Conserved protein sequences containing aromatic side chain amino acid residues, such as phenylalanine, are usually recognized as protein binding hot spots and are likely to be protein-protein interaction surfaces and consequently potential targets for rational drug design [32]. Therefore, our results demonstrate that new sperm motility inhibitors that selectively bind EPPIN's residues Cys102, Tyr107, and Phe117 could be developed as potential male contraceptive drugs.

REFERENCES

1. Tsuruta J, Dayton P, Gallippi C, O'Rand M, Streicker M, Gessner R, Gregory T, Silva E, Hamil K, Moser G, Sokal D. Therapeutic ultrasound as a potential male contraceptive: power, frequency and temperature required to deplete rat testes of meiotic cells and epididymides of sperm

determined using a commercially available system. Reprod Biol Endocrinol 2012; 10:7.
2. Tash JS, Attardi B, Hild SA, Chakrasali R, Jakkaraj SR, Georg GI. A novel potent indazole carboxylic acid derivative blocks spermatogenesis and is contraceptive in rats after a single oral dose. Biol Reprod 2008; 78: 1127–1138.
3. Tash JS, Chakrasali R, Jakkaraj SR, Hughes J, Smith SK, Hornbaker K, Heckert LL, Ozturk SB, Hadden MK, Kinzy TG, Blagg BSJ, Georg GI. Gamendazole, an orally active indazole carboxylic acid male contraceptive agent, targets HSP90AB1 (HSP90BETA) and EEF1A1 (eEF1A), and stimulates Il1a transcription in rat Sertoli cells. Biol Reprod 2008; 78: 1139–1152.
4. Chung SSW, Wang X, Roberts SS, Griffey SM, Reczek PR, Wolgemuth DJ. Oral administration of a retinoic acid receptor antagonist reversibly inhibits spermatogenesis in mice. Endocrinology 2011; 152:2492–2502.
5. Sexton JZ, Danshina PV, Lamson DR, Hughes M, House AJ, Yeh LA, O'Brien DA, Williams KP. Development and implementation of a high throughput screen for the human sperm-specific isoform of glyceraldehyde 3-phosphate dehydrogenase (GAPDHS). Curr Chem Genomics 2011; 5: 30–41.
6. O'Rand MG, Widgren EE, Hamil KG, Silva EJ, Richardson RT. Epididymal protein targets: a brief history of the development of epididymal protease inhibitor as a contraceptive. J Androl 2011; 32: 698–704.
7. O'Rand MG, Widgren EE, Sivashanmugam P, Richardson RT, Hall SH, French FS, VandeVoort CA, Ramachandra SG, Ramesh V, Jagannadha Rao A. Reversible immunocontraception in male monkeys immunized with Eppin. Science 2004; 306:1189–1190.
8. Lishko PV, Kirichok Y, Ren D, Navarro B, Chung J-J, Clapham DE. The control of male fertility by spermatozoan ion channels. Annu Rev Physiol 2012; 74:453–475.
9. McCrudden MT, Dafforn TR, Houston DF, Turkington PT, Timson DJ. Functional domains of the human epididymal protease inhibitor, eppin. FEBS J 2008; 275:1742–1750.
10. Yenugu S, Richardson RT, Sivashanmugam P, Wang Z, O'Rand MG, French FS, Hall SH. Antimicrobial activity of human EPPIN, an androgen-regulated, sperm-bound protein with a whey acidic protein motif. Biol Reprod 2004; 71:1484–1490.
11. Wang Z, Widgren EE, Richardson RT, O'Rand MG. Characterization of an Eppin protein complex from human semen and spermatozoa. Biol Reprod 2007; 77:476–484.
12. Wang Z, Widgren EE, Sivashanmugam P, O'Rand MG, Richardson RT. Association of Eppin with semenogelin on human spermatozoa. Biol Reprod 2005; 72:1064–1070.
13. Mitra A, Richardson RT, O'Rand MG. Analysis of recombinant human semenogelin as an inhibitor of human sperm motility. Biol Reprod 2010; 82:489–496.
14. O'Rand MG, Widgren EE, Beyler S, Richardson RT. Inhibition of human sperm motility by contraceptive anti-Eppin antibodies from infertile male monkeys: effect on cyclic adenosine monophosphate. Biol Reprod 2009; 80:279–285.
15. O'Rand MG, Widgren EE, Wang Z, Richardson RT. Eppin: an effective target for male contraception. Mol Cell Endocrinol 2006; 250:157–162.
16. O'Rand MG, Widgren EE. Loss of calcium in human spermatozoa via EPPIN, the semenogelin receptor. Biol Reprod 2012; 86:55, 51–57.
17. Eglen RM, Reisine T, Roby P, Rouleau N, Illy C, Bosse R, Bielefeld M. The use of AlphaScreen technology in HTS: current status. Curr Chem Genomics 2008; 1:2–10.
18. Wilson J, Rossi CP, Carboni S, Fremaux C, Perrin D, Soto C, Kosco-Vilbois M, Scheer A. A homogeneous 384-well high-throughput binding assay for a TNF receptor using alphascreen technology. J Biomol Screen 2003; 8:522–532.
19. Arnold K, Bordoli L, Kopp J, Schwede T. The SWISS-MODEL workspace: a web-based environment for protein structure homology modelling. Bioinformatics 2006; 22:195–201.
20. Schwede T, Kopp J, Guex N, Peitsch MC. SWISS-MODEL: an automated protein homology-modeling server. Nucleic Acids Res 2003; 31: 3381–3385.
21. Bordoli L, Kiefer F, Arnold K, Benkert P, Battey J, Schwede T. Protein structure homology modeling using SWISS-MODEL workspace. Nat Protocols 2008; 4:1–13.
22. Benkert P, Biasini M, Schwede T. Toward the estimation of the absolute quality of individual protein structure models. Bioinformatics 2011; 27: 343–350.
23. Richardson RT, Sivashanmugam P, Hall SH, Hamil KG, Moore PA, Ruben SM, French FS, O'Rand M. Cloning and sequencing of human Eppin: a novel family of protease inhibitors expressed in the epididymis and testis. Gene 2001; 270:93–102.
24. Parkin S, Rupp B, Hope H. Structure of bovine pancreatic trypsin inhibitor at 125 K definition of carboxyl-terminal residues Gly57 and Ala58. Acta Crystallogr D Biol Crystallogr 1996; 52:18–29.
25. Krowarsch D, Cierpicki T, Jelen F, Otlewski J. Canonical protein inhibitors of serine proteases. Cell Mol Life Sci 2003; 60:2427–2444.
26. Cassel JA, Blass BE, Reitz AB, Pawlyk AC. Development of a novel nonradiometric assay for nucleic acid binding to TDP-43 suitable for high-throughput screening using AlphaScreen® technology. J Biomol Screen 2010; 15:1099–1106.
27. Zhang J-H, Chung TDY, Oldenburg KR. A simple statistical parameter for use in evaluation and validation of high throughput screening assays. J Biomol Screen 1999; 4:67–73.
28. Wang Z, Widgren EE, Richardson RT, Orand MG. Eppin: a molecular strategy for male contraception. Soc Reprod Fertil Suppl 2007; 65: 535–542.
29. Sivashanmugam P, Hall SH, Hamil KG, French FS, O'Rand MG, Richardson RT. Characterization of mouse Eppin and a gene cluster of similar protease inhibitors on mouse chromosome 2. Gene 2003; 312: 125–134.
30. Clauss A, Lilja H, Lundwall A. A locus on human chromosome 20 contains several genes expressing protease inhibitor domains with homology to whey acidic protein. Biochem J 2002; 368:233–242.
31. Clauss A, Persson M, Lilja H, Lundwall A. Three genes expressing Kunitz domains in the epididymis are related to genes of WFDC-type protease inhibitors and semen coagulum proteins in spite of lacking similarity between their protein products. BMC Biochem 2011; 12:55.
32. Ma B, Nussinov R. Trp/Met/Phe hot spots in protein-protein interactions: potential targets in drug design. Curr Top Med Chem 2007; 7:999–1005.